Journal of Sensor Science and Technology
Vol. 25, No. 2 (2016) pp. 103-109
http://dx.doi.org/10.5369/JSST.2016.25.2.103
pISSN 1225-5475/eISSN 2093-7563

Recent Trends of Light-enhanced Metal Oxide Gas Sensors: Review

Minkyu Cho and Inkyu Park[+]

Abstract

Recent light-enhanced metal oxide gas sensors are reviewed in this article. The basic mechanisms of a light-enhanced metal oxide gas sensor are discussed. Many literatures reveal that the standalone sensitivity and the response/recovery time enhancements enabled by the exposing light are not as high as the performance enhancement provided by external heating. Therefore, both optimal amount of external heating and exposed light intensity are necessary to increase the performance of these light-enhanced gas sensors. The development of highly light sensitive materials and structures is important to lower the overall power consumptions of the sensors.

Keywords: Chemical sensors, metal oxide, photo-enhancement, light-enhanced gas sensors

1. INTRODUCTION

Miniaturized gas sensors have been widely used today owing to their compact size, low-power consumption, and low cost, thus making them a good choice for mobile, wearable and internet of things (IoT) applications. Particularly, metal oxide gas sensors in this category show promising performances in terms of sensitivity and response speed while having a low manufacturing cost. However, these types of sensors generally operate at high temperatures above 2-300°C to activate the chemisorption of atmospheric oxygen on the metal oxide surface [1-4]. This high operating temperature increases power consumption of the gas sensors and therefore these sensors are not suitable for the usage in hazardous environments containing explosive or flammable gas species [3,5]. Additionally, the high operating temperature degrades the stability of the sensor materials and structures. It has been reported that the sensors operating at high temperatures have long-term drift problems due to the diffusion and sintering processes [1,3]. Therefore, it is necessary to reduce the operating temperature of the gas sensors while maintaining their stability and sensitivity. Light irradiation is one of the methods to improve the gas sensitivity at low operating temperatures. In this article, recent works on the light-enhanced gas sensors operating at low or room temperatures were reviewed. Since each light-enhanced gas sensor uses different materials, synthesis methods, gas species, gas concentrations, and light sources, direct performance comparisons among the gas sensors were not made. Instead, this article focused on the recent trends of the light-enhanced gas sensors and their light sources, providing a guidance on the potential light-enhanced gas sensor researches in the future.

Department of Mechanical Engineering, Korea Advanced Institue of Science and Technology (KAIST), 291 Daehak-ro, Yoosung-Gu, Daejeon 305-701, Korea
[+]Corresponding author: inkyu@kaist.ac.kr
(Received: Mar. 23, 2016, Accepted: Mar. 29, 2016)

2. LIGHT-ENHANCED GAS SENSORS

2.1 Metal oxide gas sensor mechanism

The complete mechanism of metal oxides gas sensing is still not clear; however, there is a consensus that the governing mechanism is based on the free charge carrier exchange between adsorbed gas species and bulk metal oxides. For example, in n-type metal oxides, electrons in the conduction band are drawn and trapped at the metal oxide surface as O_2 is adsorbed. As a result, a band bending occurs at the surface. The band bending region is called the space-charge layer or depletion region where almost no free charge carriers are left. The space-charge layer thickness is modulated as adsorbed O_2 reacts with other gas species, and this modulation leads to conductivity change in the metal oxides. The conductivity change by gas exposure not only depends on the sensing material properties but also on the geometries when the nanocrystal size is larger than Debye length (L_D) of an electron

Table 1. List of light-enhanced metal oxide gas sensors

Material	Target Gas	Gas conc. (ppm)	Temp. (°C)	Light Source	Note	Ref.
CdS/ZnO	Formaldehyde	10	RT	450-nm, 500-W Xe-lamp	$\frac{\Delta I}{I_g}(100\%) = 120\%$	[13]
ZnO	Ethylene, Acetone	5200 (Ethylene) 900 (Acetone)	RT	4-W white-LED (380–780 nm)	$\frac{R_a}{R_g} = 1.06$ (Ethylene), 1.2 (Acetone)	[1]
ZnO (Sn doped)	Ethanol	320	RT	Visible-light (not specified)	$\frac{R_a}{R_g}(100) = 225\%$	[2]
ZnO	Acetone, Toluene, Pentane, Acetaldehyde	0.001 – 10	RT	400-nm UV-LED (2.2 mW/cm^2)	Response not specified, able to detect <100 ppb for all test gas	[14]
ZnO (TiO_2 doped)	Ethanol	50-200	RT	365-nm, 24-W UV lamp	5 wt% TiO_2 doped performed best	[10]
ZnO (Cu doped)	Ethanol, Acetone	1120	RT	355-nm Xe-lamp	$\frac{\Delta I}{I_g}(100\%) = 64\%$ (ethanol), 63% (acetone)	[20]
ZnO (Au coated)	NO_2	5	RT	365 nm (1.2 mW/cm^2)	455%	[21]
ZnO	H_2,	100	RT	UV irradiation (not specified)	$\frac{\Delta R}{R_g} = 0.56$	[22]
SnO_2/ZnO	NO_2	5	RT	365 nm (1.2 mW/cm^2)	619%	[4]
ZnO	H_2	100	RT	365 nm UV-LED (25 mW/cm^2)	$\frac{\Delta R}{R_g} = 0.2$	[16]
SnO_2/TiO_2	Ethanol	100	RT	380 nm UV-LED (0.7 Cd/m^2 by 2 mm apart)	$\frac{R_a}{R_g}(100) = 16$	[3]
SnO_2	NO_2	1–3	RT - 300	365 nm, Mercury-Xe lamp (3500 mW/cm^2)	$\frac{\Delta R}{R_g} = 90\%$ (300°C, 3 ppm)	[5]
SnO_2 (Au, In, Si doped)	CO	100	0 - 500	365 nm, Mercury-Xe lamp(15 mW/m^2)	$\frac{\Delta R}{R_g} = 1$ (Au doped, 300°C), 0.8 (undoped, 300°C), 0.6 (In doped, 300°C), 0.5 (Si doped, 400°C)	[15]
WO_3	NO_2	0.16 – 0.32	RT	380, 400, 480, 510, 590 nm LEDS	$\frac{R_{NO_2}}{R_{air}} = 9.2$ (max. response under 590 nm at RT)	[9]
ZnS (Au doped)	NO_2	5	300	254 nm LED 1.2 mW/cm^2	884%	[8]

[6]. These well-known metal oxide materials for gas sensors are the transition-metal oxides with d^0 and d^{10} electronic configurations such as TiO_2, V_2O_5, WO_3, ZnO, and SnO_2 [7].

2.2 Light-enhanced metal oxide gas sensor mechanism

The mechanism of light-enhanced metal oxides is essentially similar to the general heat-operated metal oxide gas sensors, but it involves photocatalytic reactions of photo-generated carriers in the gas adsorption/desorption process. The governing mechanism of light-enhanced gas sensors can be summarized as follows:

1. Increased free charge carrier density in metal oxides due to generated electron-hole pairs by light illuminations.
2. Weakly bound oxygen species on the metal oxide surfaces formed by cyclic reactions between oxide species and photo-generated electron-hole pairs.

Graphic illustrations of the light-assisted gas sensing mechanism are shown in Fig. 1 [1].Under the dark condition, the chemisorbed oxygen species are strongly bound to the metal oxides surfaces in the oxygen-ambient atmosphere [Fig.. 1(a)]. As the light is illuminated to the metal oxides, the chemisorbed oxygen species are desorbed by interacting with photo-generated

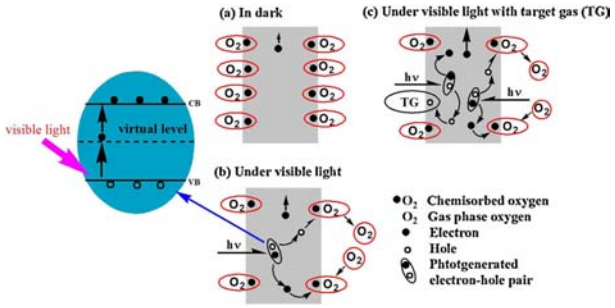

Fig. 1. Graphic illustrations describing the mechanism of light-enhanced metal oxide gas sensors (adapted from [1]).

electrons [Fig. 1(b)]. By oxygen desorption, the space-charge layer thickness is reduced increasing the conductivity of the metal oxides. After desorption of chemisorbed oxygen species, the new oxygen species are adsorbed by interacting with photo-generated electrons and the conductivity is decreased. Unlike chemisorbed oxygen species, the new oxygen species are weakly bound to the surface so that the absorption/desorption process could be activated at low temperatures. The absorption/desorption process soon reaches the steady state after a while. Upon target gas exposure, for example of reducing gas, the photo-generated holes are recombined to the electrons donated from the target gas causing the electron-hole separation, and this leads to the decrease in the resistance across the metal oxides [Fig 1(c)].

2.2 Photo-generated free charge carriers in light-enhanced metal oxide gas sensors

The free charge carrier generation by light illumination in the metal oxides is explained by the principle of interband transition. When light is irradiated to the metal oxides, the electrons in the valence band are excited to the conduction band forming electron-hole pairs. Only the light that has higher energy than the band gap of the metal oxides can generate electron-hole pairs in the interband transition. Fig. 4 (d) shows the relation between the gas sensing responses and the photon energy (wavelength). It is observed that the gas response rapidly increases when the light energy is higher than the band gap (SnO_2 in the figure) of the sensing material. For this reason, UV light ($\lambda < 400$ nm) is usually used as the light source for the metal oxide gas sensors.

Recent light-enhanced gas sensors and their sensitivities to different target gases are listed in Table 1. Some of the light-enhanced gas sensors improve their responses by adding different materials to the metal oxides surfaces. S. Park et al. synthesized 1D ZnS nanostructures on the Au-coated sapphire (001) substrate, sputtered Au thin film to the nanowires, and the Au-functionalized ZnS nanowires gas sensor was fabricated [8]. The TEM image of an Au-functionalized ZnO nanowire is shown in Fig 2 (a). In response to 1, 2, 3, 4, and 5 ppm NO_2 gas, these Au-functionalized ZnS nanowire gas sensors showed superior responses of up to 2.8, 3.3, 3.6, 5.1, 5.4-fold, respectively [Fig. 2 (b)], compared to the responses of pristine ZnO nanowire gas sensors. Another work by S. Park et al. reported light-enhanced SnO_2-core/ZnO-shell nanowire gas sensor structures using a two-step process: the synthesis of SnO_2 nanowires was followed by atomic layer deposition (ALD) of ZnO [4]. The response of the SnO_2-core/ZnO-shell gas sensors is 618% in 5 ppm NO_2 under 1.2 mW/cm^2 UV illumination. This response is a huge improvement compared to the responses of pristine ZnO and SnO_2 nanowire gas sensors in the same conditions. The reason for the improved responses of these core-shell structures is because the n-n heterojunction acts as a lever through which the electron transfer rate is controlled [4]. The band diagrams of the SnO_2/ZnO core-shell structure before and after equilibrium, with and without UV irradiation are described in Fig. 2 (d). J.D. Prades et al. reported on a room temperature light-enhanced monocrystalline SnO_2 nanowire gas sensor as shown in Fig. 4 (a) [9]. Under UV illumination, their sensor demonstrated detection as low as 100 ppb NO_2 at room temperature [Fig. 4. (b)]. The improvement in light-enhanced gas sensors' responses by changing the wt% of the doping materials was reported in [10]. In UV spectra, the ZnO doped with a small TiO_2 contents exhibited red-shift, and the ZnO doped with large TiO_2 contents exhibited blue-shift [Fig. 2 (j)]. They found the highest gas sensing response when ZnO is doped with 5 wt% of TiO_2 as shown in Fig. 2 (k). A high gas sensitivity is observed when the spectra is red-shifted because most of the materials have a higher absorption coefficient in longer wavelengths.

Most light-enhanced gas sensors require light sources to be activated. However, these light sources lie in UV range and have high power consumption. Therefore, there have been many attempts to use visible light sources, which are more ambient and less power-consuming, to generate the electron-hole pairs in the metal oxide gas sensors. Q. Geng et al. revealed that ZnO gas sensors could respond to the visible light [1] produced by the two-photon excitation process [11, 12] so that the visible light can be used as an excitation source. C. Shao et al. found that changing the concentration of Sn in the Zn:Sn source material would control the number of defects in ZnO, and that these defects work as electron donors allowing ZnO to absorb visible light [2]. They also found that with 1:1 Zn:Sn ratio (denoted as SZ2), the defects concentration is the highest, and therefore the maximum gas response is achieved

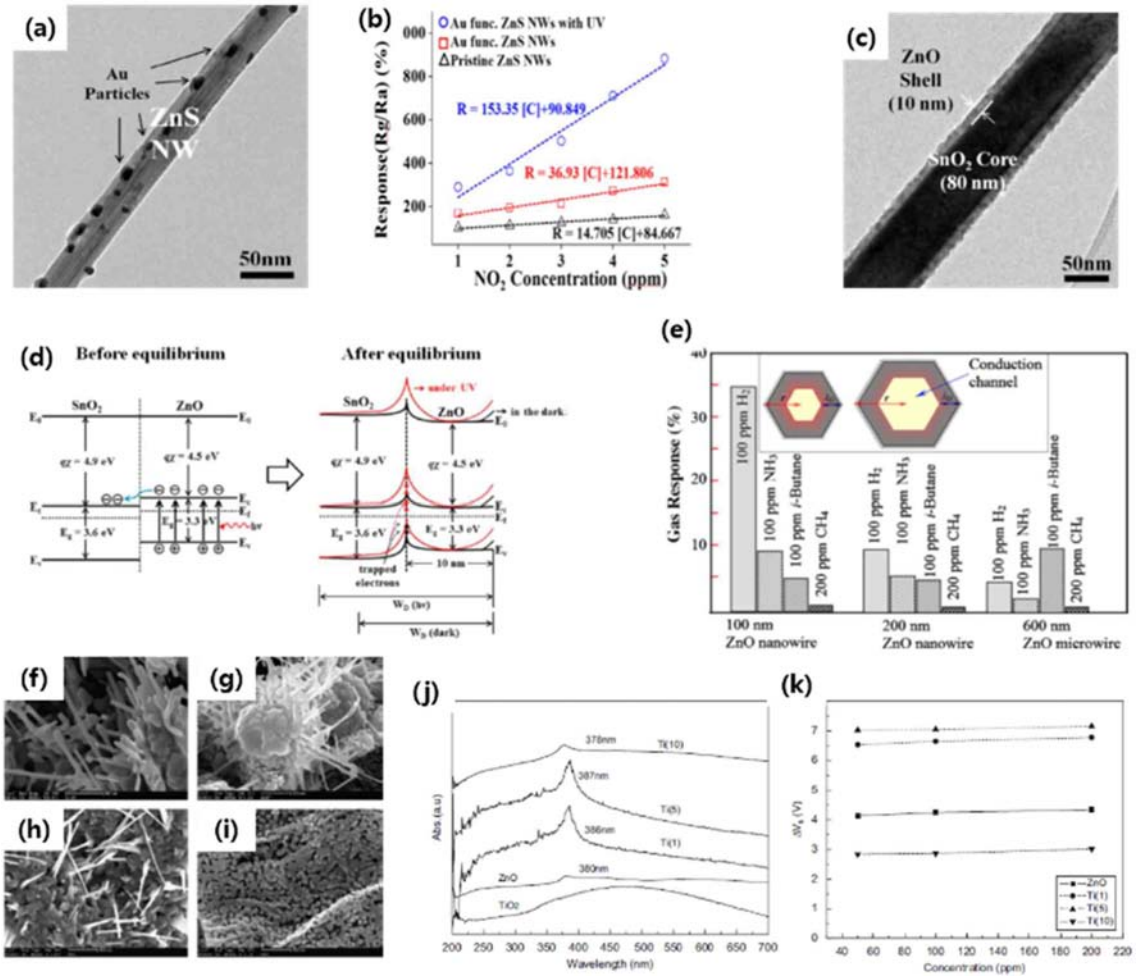

Fig. 2. (a) TEM image of Au-coated ZnS NW, (b) gas response versus NO_2 concentration for pristine ZnS NW (w/ UV) and Au-coated ZnS (w/o UV), Au-coated ZnS (w/ UV), adapted from [8]. (c) TEM image of SnO_2-core/ZnO-shell NW. (d) Energy band diagrams of SnO_2-core/ZnO-shell NW before and after equilibrium (with and without UV), adapted from [4]. (e) H_2, NH_3 i-Butane, CH_4 gas responses of ZnO NW light-enhanced gas sensors with different diameters, adopted from [22]. SEM images of ZnO specimens: (f) Prinstine ZnO, (g) 1 wt% TiO_2-doped ZnO, (h) 5wt% TiO_2-doped ZnO, (i) 10wt% TiO_2-doped ZnO. (j) Absorption spectra and (k) ethanol vapor response of pristine ZnO sample and ZnO samples doped with different TiO_2 concentrations (1, 5, 10 wt%). Fig. 2. (f-k) was adapted from [10].

[Fig. 3(e)]. Fig. 3 shows the SEM images of ZnO samples with different Sn concentrations (a-c) and the corresponding UV spectra [2]. A light-enhanced gas sensor incorporated both CdS, which have a band gap ~2.4 eV, and ZnO was also reported to enhance the visible light responses [13].

2.3 Operation condition optimization (light intensity and temperature) for light-enhanced metal oxide gas sensors

Because each light-enhanced gas sensor has different material preparation methods, device structures, and illuminated light conditions, the question of the best operating conditions is still debated by researchers. Several works reported that the maximum response is achieved by a moderate light intensity. J.D Predas et al. demonstrated experimentally that the response is a function of both photon flux and gas concentration in their SnO_2 nanowire gas sensors as shown in Fig. 4 (c) [9]. Based on their study, the maximum gas response is obtained with photon flux, enough for desorbed oxygen to create new oxygen vacancies but not excessive to prevent large desorption of NO_2. In a light-enhanced ZnO gas sensor study, B.P.J. Costello et al. found that the optimal light intensity giving maximum response is dependent on the analyte [14]. Fig. 5 (a-d) show the sensor responses versus light intensities for different gas types (hexane, propane, methane, and ethanol). To find out the optimal temperature for light-enhanced gas sensors, E. Comini et al. investigated the relationship between the gas sensor sensitivity and the temperature under light

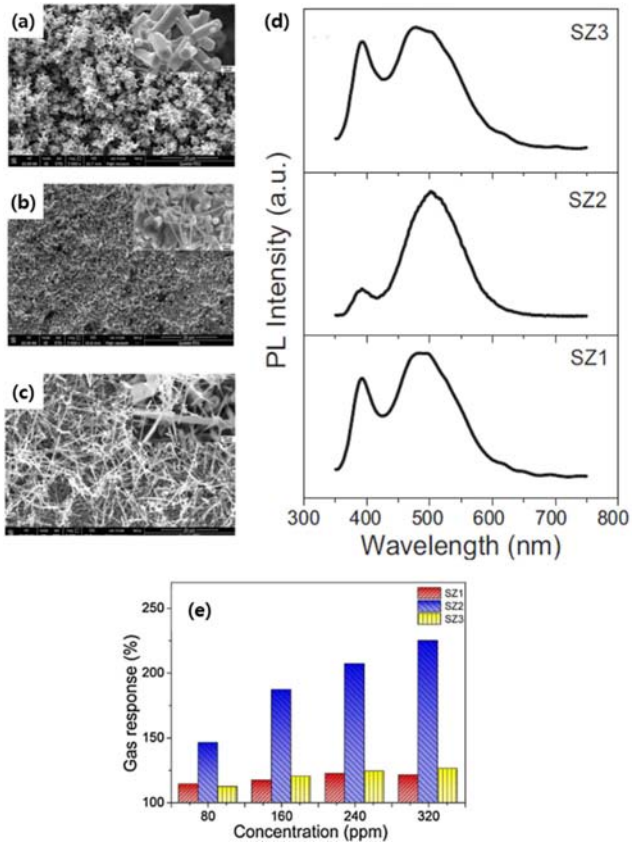

Fig. 3. (a-c) SEM images, (d) room-temperature PL spectra of Zn:Sn: 2:3, 1:1, 1:3 (from top to bottom). (e) Ethanlol vapor responses of the samples prepared with different weight ratio Zn:Sn, All adapted from [2].

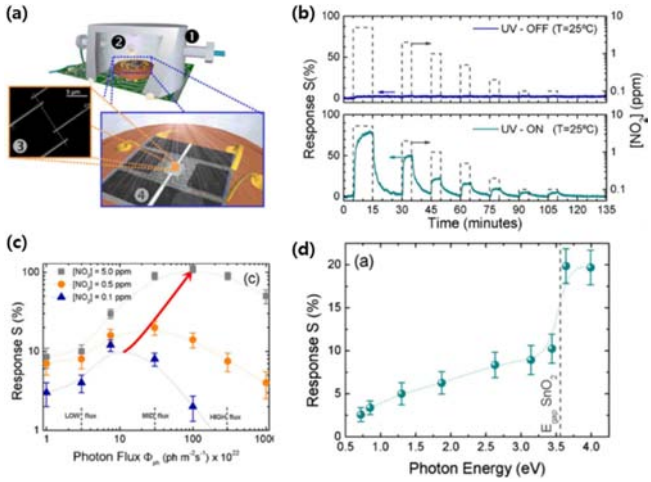

Fig. 4. (a) Schematic representation of the nanowire device and experimental setup, (b) response of a SnO_2 NW operated in dark and UV illuminated to NO_2 of different concentrations. (c) Sensor response of the SnO_2 NW devices under illumination with different photon energies and photon flux towards 0.5-ppm NO_2. (d) Variation of sensor response for three different concentration of NO_2 vs. the flux of photons. All figures are adapted from [9].

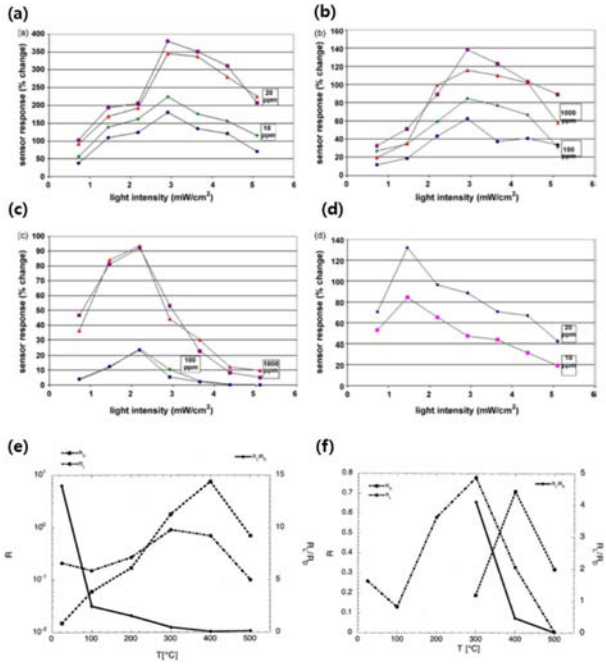

Fig. 5. Plot of sensitivity (% change in baseline current) vs. light intensity when nanoparticulate zinc oxide sensors were exposed to (a) hexane vapor, (b) propane vapor, (c) methane vapor, (d) ethanol vapor. Reponse in dark- and UV-irradiation condition for (e) gold catalyzed and (f) pristine SnO_2 RGTO samples as a function of the working temperature towards 100 ppm of CO at 30% RH. (a-d) were adapted from [14], and (e, f) were adapted from [15].

illumination [15], and measured the highest responses of light illuminated gas sensors at a working temperature of 300°C [Fig. 5 (e, f)]. Moreover, they found a memory effect occurred when their sensors are operated in low incident power and low temperature, but the effect is eliminated as the working temperature is increased above 250°C.

2.3 Challenge in light-enhanced metal oxide gas sensors

The light source is a challenge in light-enhanced gas sensors. Bulky and high power light sources cancel out the small form factors of nanofabricated gas sensors. There were attempts to use low power LEDs with the gas sensors [3,16], but the light source and gas sensor were two separate parts. Therefore, combining both the light sources and gas sensors in one platform is desirable for future integration with mobile/wearable device applications. We believe that the advanced fabrication methods such as focused energy field method [17], high-resolution electrohydrodynamic (EHD) printing [18] or nanomembrane transfer printing [19] would make it possible to integrate both light source and gas sensor in a single small platform (Fig. 6).

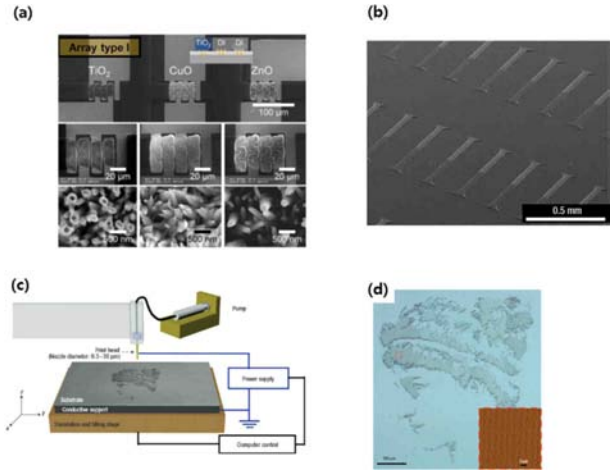

Fig. 6. (a) Images of heterogeneous nanomaterial array consisting of TiO_2 nanotubes, CuO nanospikes, and ZnO nanowires grown on micro heater platforms (adapted from [17]). (b) Silicon photodiodes printed on a spherical glass surface by transfer printing (adapted from [19]). (c) Electrohydrodynamic jet printer setup. (d) Optical micrograph of portrait of the ancient scholar, Hypatia, printed using a polyurethane ink and 500 nm internal diameter nozzle. (c, d) were adapted from [18].

3. CONCLUSIONS

In this article, various light-enhanced metal oxide sensors were reviewed. In the first two sections of this article, the basic mechanisms of light-enhanced gas sensors were explained. We then introduced some of the recent publications and their attempts, which demonstrated the absorption wavelength tuning methods and operating condition optimizations, to improve the light-enhanced gas sensor's performance.

ACKNOWLEDGMENT

This work was supported by the National Research Foundation of Korea (NRF) Grant funded by the Korean Government (MSIP) (No. 2015R1A5A1037668), the Center for Integrated Smart Sensors funded by the Ministry of Science, ICT & Future Planning as Global Frontier Project (CISS-2012M3A6A6054201), and by the BK21 Plus Program.

REFERENCES

[1] Q. Geng, Z. He, X. Chen, W. Dai, and X. Wang, "Gas sensing property of ZnO under visible light irradiation at room temperature", *Sens. Actuators, B*, Vol. 188, pp. 293-297, 2013.

[2] C. Shao, Y. Chang, and Y. Long, "High performance of nanostructured ZnO film gas sensor at room temperature", *Sens. Actuators, B*, Vol. 204, pp. 666-672, 2014.

[3] J. Sun, J. Xu, Y. Yu, P. Sun, F. Liu, and G. Lu, "UV-activated room temperature metal oxide based gas sensor attached with reflector", *Sens. Actuators, B*, Vol. 169, pp. 291-296, 2012.

[4] S. Park, S. An, Y. Mun, and C. Lee, "UV-Enhanced NO2 gas sensing properties of SnO_2-Core/ZnO-shell nanowires at room temperature", *ACS Appl. Mater. Interfaces*, Vol. 5, pp. 4285-4292, 2013.

[5] E. Comini, G. Faglia, and G. Sberveglieri, "UV light activation of tin oxide thin films for NO_2 sensing at low temperatures", *Sens. Actuators, B*, Vol. 78, pp. 73-77, 2001.

[6] W. Göpel and K. D. Schierbaum, "SnO_2 sensors: current status and future prospects", *Sens. Actuators, B*, Vol. 26, pp. 1-12, 1995.

[7] C. Wang, L. Yin, L. Zhang, D. Xiang, and R. Gao, "Metal oxide gas sensors: Sensitivity and influencing factors", Sensors, Vol. 10, p. 2088, 2010.

[8] S. Park, S. An, H. Ko, S. Lee, and C. Lee, "Synthesis, structure, and UV-enhanced gas sensing properties of Au-functionalized ZnS nanowires", *Sens. Actuators, B*, Vol. 188, pp. 1270-1276, 2013.

[9] J. D. Prades, R. Jimenez-Diaz, F. Hernandez-Ramirez, S. Barth, A. Cirera, A. Romano-Rodriguez, et al., "Equivalence between thermal and room temperature UV light-modulated responses of gas sensors based on individual SnO_2 nanowires", *Sens. Actuators, B*, Vol. 140, pp. 337-341, 2009.

[10] Y. Gui, S. Li, J. Xu, and C. Li, "Study on TiO_2-doped ZnO thick film gas sensors enhanced by UV light at room temperature", *Microelectron. J.*, Vol. 39, pp. 1120-1125, 2008.

[11] J.-H. Lin, Y.-J. Chen, H.-Y. Lin, and W.-F. Hsieh, "Two-photon resonance assisted huge nonlinear refraction and absorption in ZnO thin films", *J. Appl. Phys.*, Vol. 97, p. 033526, 2005.

[12] C. F. Zhang, Z. W. Dong, G. J. You, R. Y. Zhu, S. X. Qian, H. Deng, et al., "Femtosecond pulse excited two-photon photoluminescence and second harmonic generation in ZnO nanowires", *Appl. Phys. Lett.*, Vol. 89, p. 042117, 2006.

[13] J. Zhai, L. Wang, D. Wang, H. Li, Y. Zhang, D. q. He, et al., "Enhancement of gas sensing properties of CdS Nanowire/ZnO nanosphere composite materials at room temperature by visible-light activation", *ACS Appl. Mater. Interfaces*, Vol. 3, pp. 2253-2258, 2011.

[14] B. P. J. de Lacy Costello, R. J. Ewen, N. M. Ratcliffe, and M. Richards, "Highly sensitive room temperature sensors based on the UV-LED activation of zinc oxide nanoparticles", *Sens. Actuators, B*, Vol. 134, pp. 945-952, 2008.

[15] E. Comini, L. Ottini, G. Faglia, and G. Sberveglieri, "SnO_2 RGTO UV activation for CO monitoring", *IEEE Sens. J.*, Vol. 4, pp. 17-20, 2004.

[16] S.-W. Fan, A. K. Srivastava, and V. P. Dravid, "UV-activated room-temperature gas sensing mechanism of polycrystalline ZnO", *Appl. Phys. Lett.*, Vol. 95, p. 142106,

2009.
[17] D. Yang, K. Kang, D. Kim, Z. Li, and I. Park, "Fabrication of heterogeneous nanomaterial array by programmable heating and chemical supply within microfluidic platform towards multiplexed gas sensing application", *Sci. Rep.*, Vol. 5, p. 8149, 2015.
[18] J.-U. Park, M. Hardy, S. J. Kang, K. Barton, K. Adair, D. k. Mukhopadhyay, et al., "High-resolution electrohydrodynamic jet printing", *Nat. Mater.*, Vol. 6, pp. 782-789, 2007.
[19] M. A. Meitl, Z.-T. Zhu, V. Kumar, K. J. Lee, X. Feng, Y. Y. Huang, et al., "Transfer printing by kinetic control of adhesion to an elastomeric stamp", *Nat. Mater.*, Vol. 5, pp. 33-38, 2006.
[20] L. Peng, T.-F. Xie, M. Yang, P. Wang, D. Xu, S. Pang, et al., "Light induced enhancing gas sensitivity of copper-doped zinc oxide at room temperature", *Sens. Actuators, B*, Vol. 131, pp. 660-664, 2008.
[21] Y. Mun, S. Park, S. An, C. Lee, and H. W. Kim, "NO2 gas sensing properties of Au-functionalized porous ZnO nanosheets enhanced by UV irradiation", *Ceram. Int.*, Vol. 39, pp. 8615-8622, 2013.
[22] O. Lupan, V. V. Ursaki, G. Chai, L. Chow, G. A. Emelchenko, I. M. Tiginyanu, et al., "Selective hydrogen gas nanosensor using individual ZnO nanowire with fast response at room temperature", *Sens Actuators, B*, Vol. 144, pp. 56-66, 2010.